Supplementary Information

Enantioselective Self-Assembly of Chiral Calix[4]arene Acid with Amines

Yan-Song Zheng,*,† Shu-Yun Ran, † Yu-Jin Hu, †and Xian-Xian Liu‡

† Department of Chemistry, Huazhong University of Science and Technology, Wuhan 430074, P. R. China, and

‡ Department of Chemistry, Guilin Normal College, Guilin, Guangxi 541001, P. R. China

zyansong@hotmail.com

Table of Contents

Materials and Methods

Materials. All reagents and solvents were chemical pure (CP) grade or analytical reagent (AR) grade and were used as received. *L*-2,3-dibenzoyltartaric anhydride was homemade by the reaction of *L*-2,3-dibenzoyltartaric acid and benzoyl chloride. *p-tert*-Butylcalix[4]arene and calix[4]arene starting materials were prepared according to supporting reference (*S1*) and (*S2*) respectively.

Measurements. ^{1}H NMR and ^{13}C NMR spectra were measured on a Bruker AV 400 spectrometer at 298 K in $CDCl_3$. Field emission scanning electron microscopy (FE-SEM) images were taken on a FEI Sirion200 electron microscope operating at 5 kV or 10 kV. The sample was prepared by casting the gel onto a glass slide and let it air dry. Transmission electron micrographs (TEM) were recorded on a FEI Technai G2 20 electron microscope at 200 kV. The gel or suspension was diluted 4 times with corresponding solvent, and then was dropped onto a copper grid covered with a thin carbon film on a filter paper and air dried. Infrared spectra were recorded on BRUKER EQUINAX55 spectrometer. Absorption spectra were recorded on a Hewlett Packard 8453 UV–Vis spectrophotometer. Fluorescent emission spectra were collected on Shimadzu RF-5301 at 298 K.

Fluorescence titration was carried out by addition of concentrated solution of chiral amine into the solution of calixarene **4** in ethanol. To keep constant concentration of calixarene **4** and account for dilution effects during titration, the solution of chiral amine was prepared with the solution of calixarene **4** at its initial concentration as a solvent.

Powder X-ray diffraction (XRD) pattern were measured on a χ'Pert PRO diffraction instrument. The scan parameters and peak list are as following:

Anchor Scan Parameters

Dataset Name:	A-4
File name:	E:\X'Pert Data\zhengyansong\20080710\A-4.xrdml
Comment:	0.5-5 degree
Measurement Date / Time:	7/10/2008 4:53:43 PM
Operator:	dell
Raw Data Origin:	XRD measurement (*.XRDML)
Scan Axis:	Gonio
Start Position [°2Th.]:	1.0084
End Position [°2Th.]:	9.9674
Step Size [°2Th.]:	0.0170
Scan Step Time [s]:	60.6901
Scan Type:	Continuous
PSD Mode:	Scanning
PSD Length [°2Th.]:	2.12
Offset [°2Th.]:	0.0000
Divergence Slit Type:	Fixed
Divergence Slit Size [°]:	0.0315
Specimen Length [mm]:	10.00
Measurement Temperature [°C]:	25.00

Anode Material:	Cu
K-Alpha1 [Å]:	1.54060
K-Alpha2 [Å]:	1.54443
K-Beta [Å]:	1.39225
K-A2 / K-A1 Ratio:	0.50000
Generator Settings:	40 mA, 40 kV
Goniometer Radius [mm]:	240.00
Dist. Focus-Diverg. Slit [mm]:	91.00
Incident Beam Monochromator:	No
Spinning:	No

Peak List

Pos.[°2Th.]	Height[cts]	FWHM[°2Th.]	d-spacing[Å]	Rel.Int.[%]
2.9988	26.54	0.5353	29.46237	11.44
5.3265	148.71	0.4684	16.59156	64.10
6.2854	232.00	0.1338	14.06228	100.00

Synthesis of calix[4]arene acid 4.

To a flask calix[4]arene **3** (0.79 g, 1.0 mmol), *L*-2,3-dibenzoyltartaric anhydride (0.78 g, 2.29 mmol) and dry THF (25 mL) were added. The mixture was stirred for about 24 h at room temperature until **3** was disappeared. The solvent was removed by rotary vaporization under reduced pressure, and the residue was recrystallized from methanol and water to afford **4** as white powders (1.05g, 93%). Mp 186–188 ^{o}C; $[\alpha]_D^{20}$ –0.377 (*c* 1.0, $CHCl_3$); IR (KBr) *v* 3306, 3041, 2959, 2869, 1732, 1603, 1483 cm^{-1}. ^{1}H NMR (400 MHz, $CDCl_3$) δ 11.64 (s, 2H, PhCOCHCON*H*), 9.45 (s, 2H, OCH_2CON*H*), 8.11–8.05 (m, 8H, OOCAr*H*), 7.90 (s, 2H, ArO*H*), 7.53–7.32 (m, 12H, OOCAr*H*), 7.02, 6.97 (2×d, *J* = 2 Hz, 4H, $ArCH_2Ar$*H*), 6.95, 6.88 (2×d, *J* = 2.5 Hz, 4H, $ArCH_2Ar$*H*), 6.01, 5.86 (2×d, *J* = 6.2 Hz, 4H, ArCOOC*H*), 5.02, 4.37 (2×d, *J* = 15 Hz, 4H, $ArOCH_2CONH$), 4.25 (d, *J* = 13.2 Hz, 2H, $ArCH_2Ar$), 4.07 (d, *J* = 13.6 Hz, 2H, $ArCH_2Ar$), 3.37 (d, *J* = 13.6 Hz, 2H, $ArCH_2Ar$), 3.32 (d, *J* = 13.2 Hz, 2H, $ArCH_2Ar$), 1.09 (s, 18H, $C(CH_3)_3$), 1.04(s, 18H, $C(CH_3)_3$); ^{13}C NMR (100 MHz, $CDCl_3$) δ 169.0, 168.1, 165.7, 165.5, 163.3, 149.2, 148.9, 148.3, 142.7, 133.8, 133.4, 132.6, 132.4, 130.3, 130.1, 128.6, 128.4, 128.3, 128.2, 127.2, 126.8, 126.3, 125.8, 125.5, 125.3, 74.1, 71.8, 71.7, 34.1, 33.8, 31.6, 30.9. Anal. Calcd for for $C_{84}H_{88}N_4O_{20}$: C, 68.45; H, 6.03; N, 3.80. Found: C, 68.32; H, 6.08; N, 3.74.

Supporting References

S1. C. D. Gutsche, M. Iqbal, D. Stewart, *J. Org. Chem.* **51**, 742 (1986).
S2. C. D. Gutsche, L. G. Lin, *Tetrahedron* **42**, 1633 (1986).

Supporting Figures

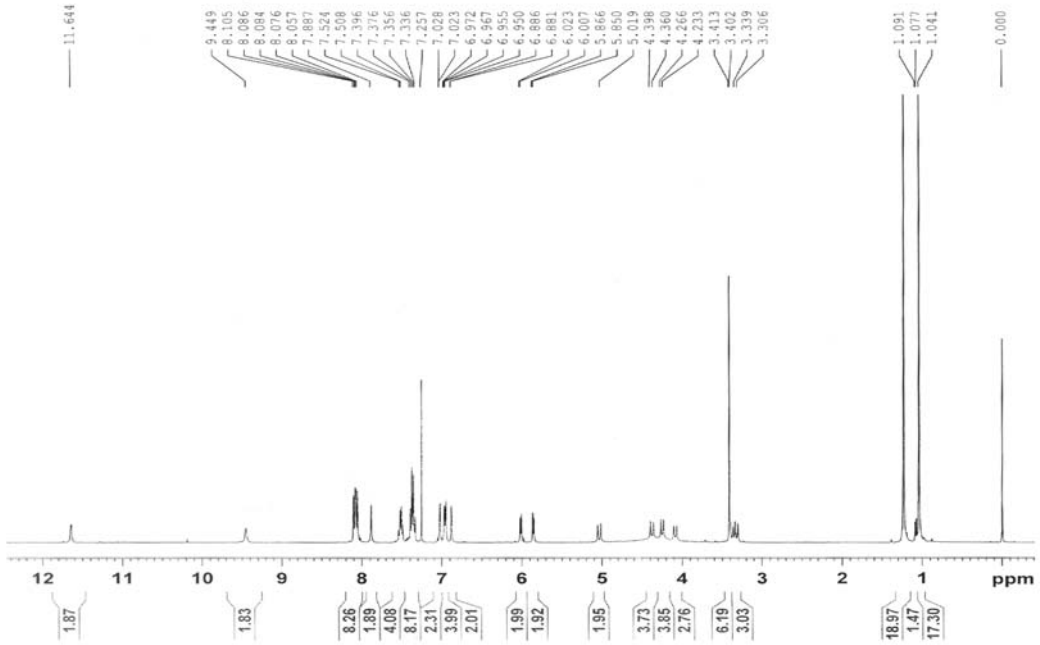

Figure S1. ^{1}H NMR spectrum of calix[4]arene acid **4** in $CDCl_3$. The high peak at 3.41 ppm is from 1,2-dichloroethane.

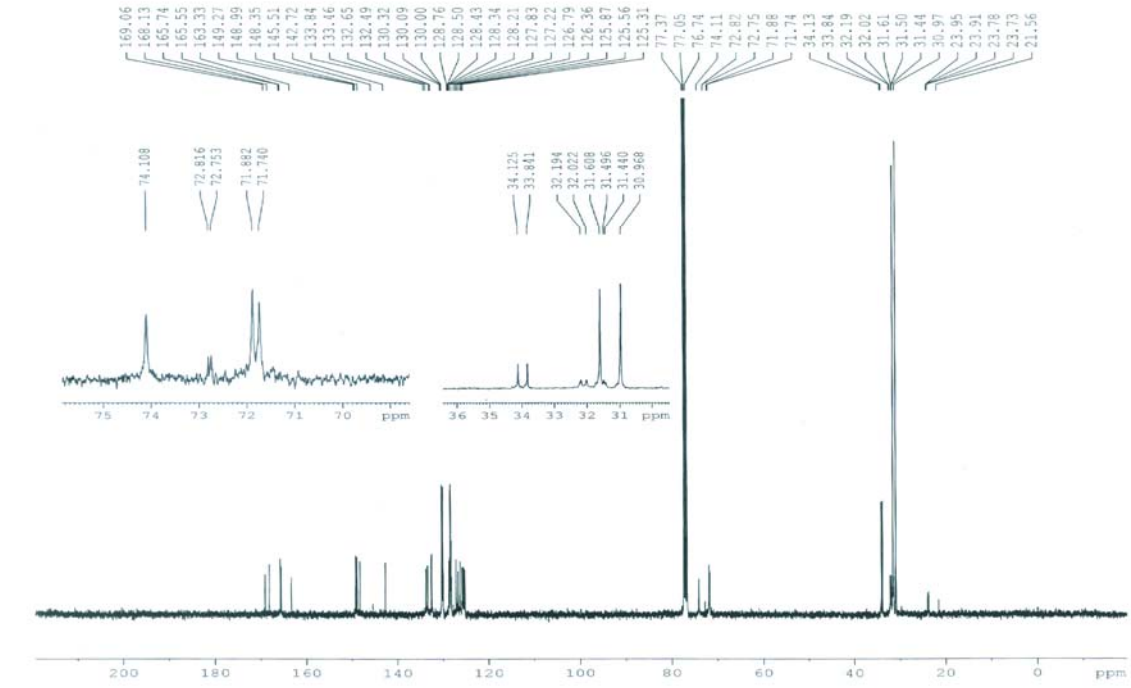

Figure S2. ^{13}C NMR spectrum of calix[4]arene acid **4** in $CDCl_3$.

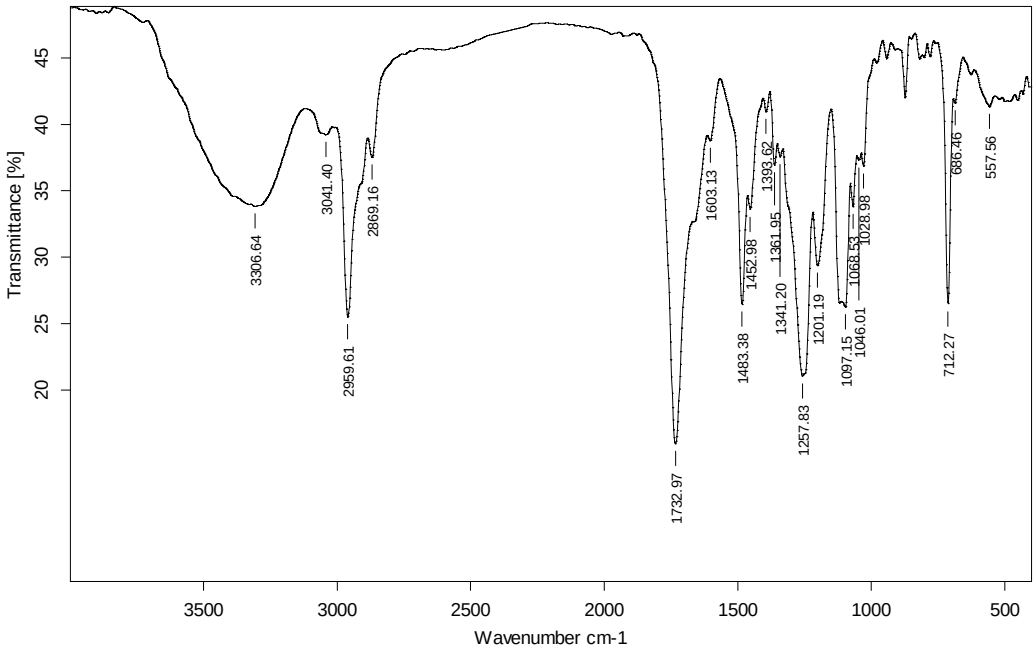

Figure S3. IR spectrum of calix[4]arene acid **4.**

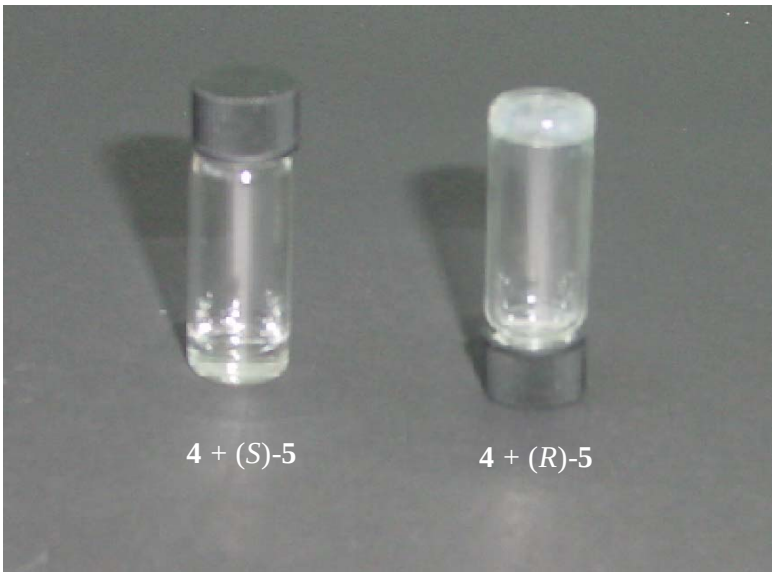

Figure S4. Gel from mixing of calix[4]arene **4** and amine (*R*)-**5** (right) in 1,2-dichloroethane, and clear solution from mixing of calix[4]arene **4** and amine (S)-**5** (left) in 1,2-dichloroethane.

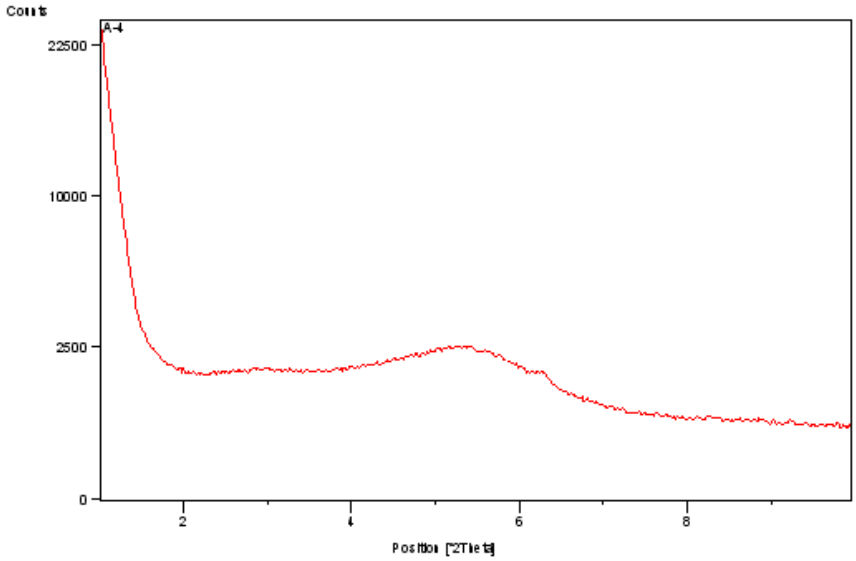

Figure S5. XRD pattern of powder solid dried from suspension of **4** and (*1S,2S*)-**8** in cyclohexane and 1,2-dichloroethane (20:1).

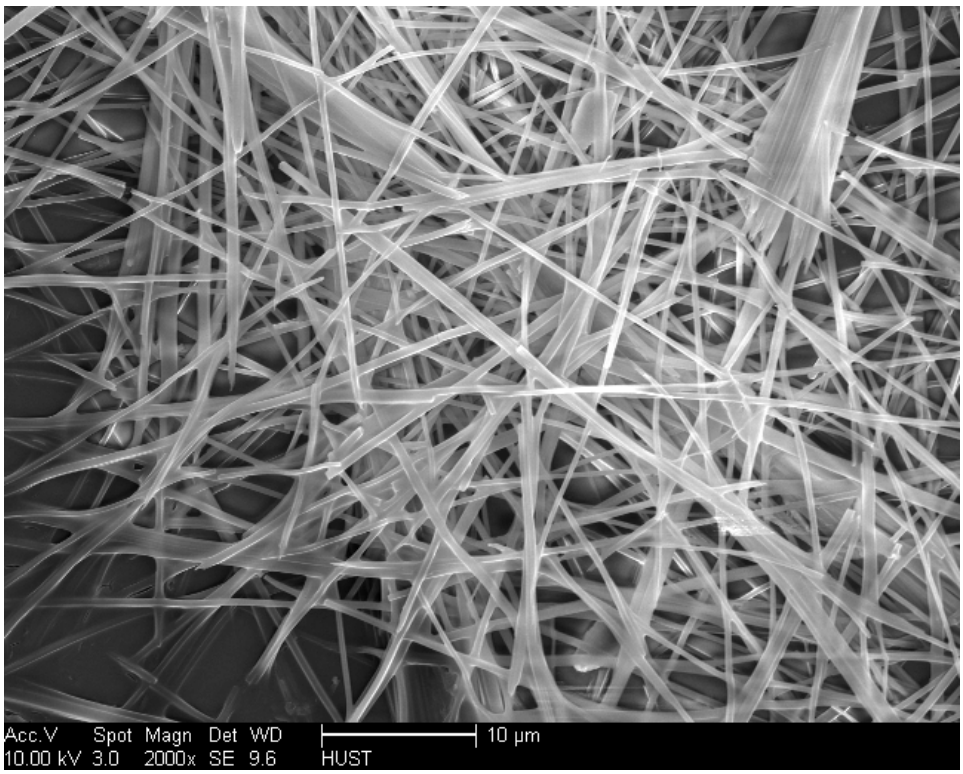

Figure S6. FE-SEM images of gel from interaction of **4** (10mM) with (*R*)-**5** (20mM) in 1,2-dichloroethane.

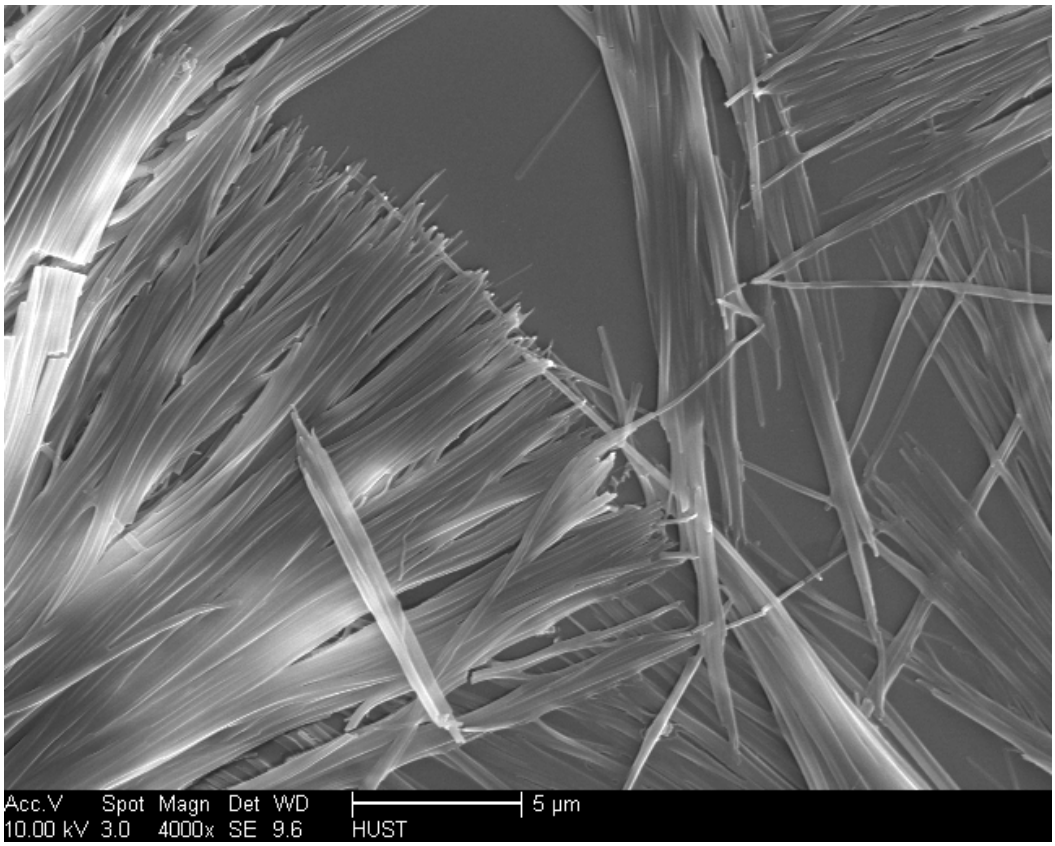

Figure S7. FE-SEM images of gel from interaction of **4** (10mM) with (*S*)-**6** (20mM) in cyclohexane and 1,2-dichloroethane of volume ratio 1:2.

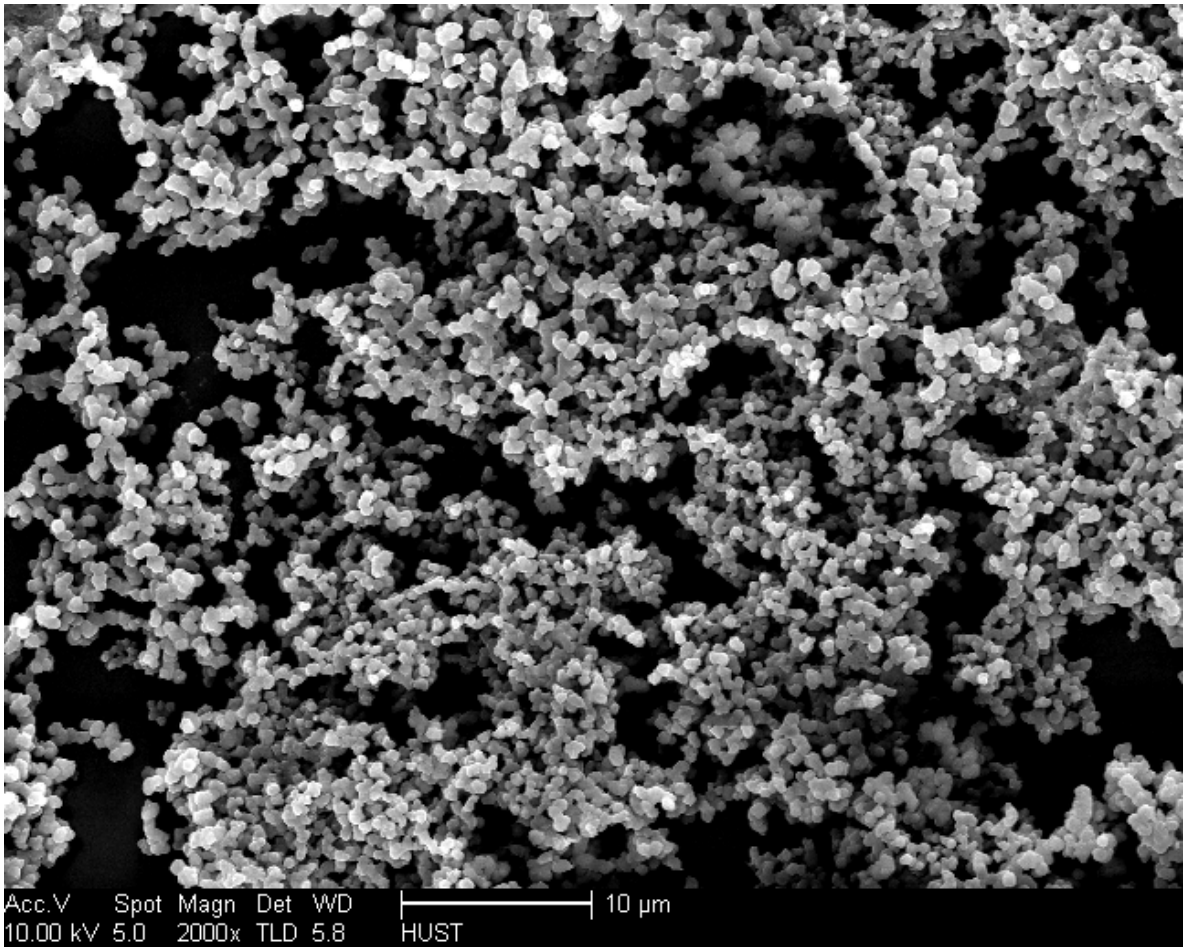

Figure S8. FE-SEM images of suspension from interaction of **4** (10mM) with (*1S,2S*)-**8** (20mM) in cyclohexane and 1,2-dichloroethane of volume ratio 20:1.

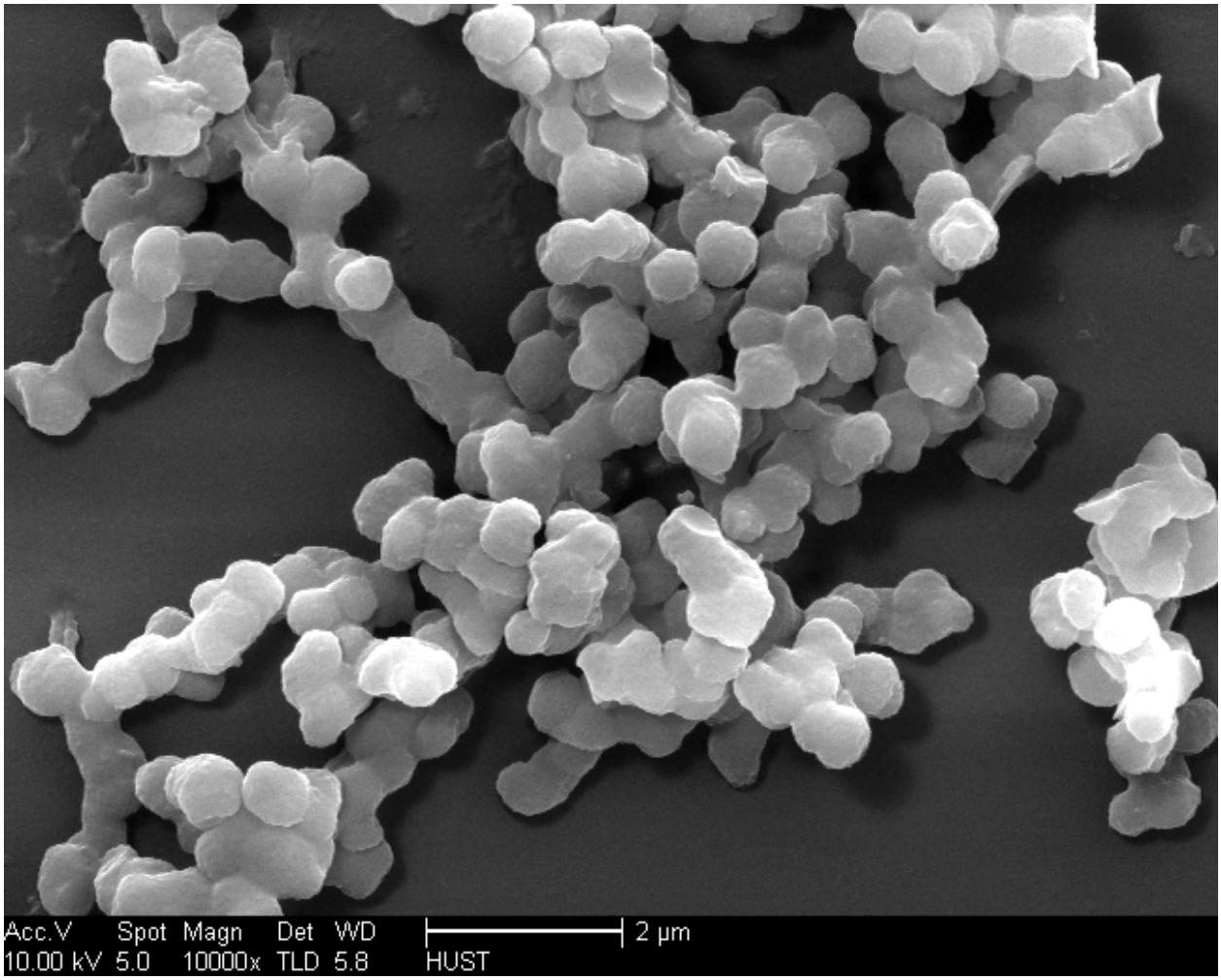

Figure S9. FE-SEM images of suspension from interaction of **4** (10mM) with (*1S,2S*)-**8** (20mM) in cyclohexane and 1,2-dichloroethane of volume ratio 20:1.

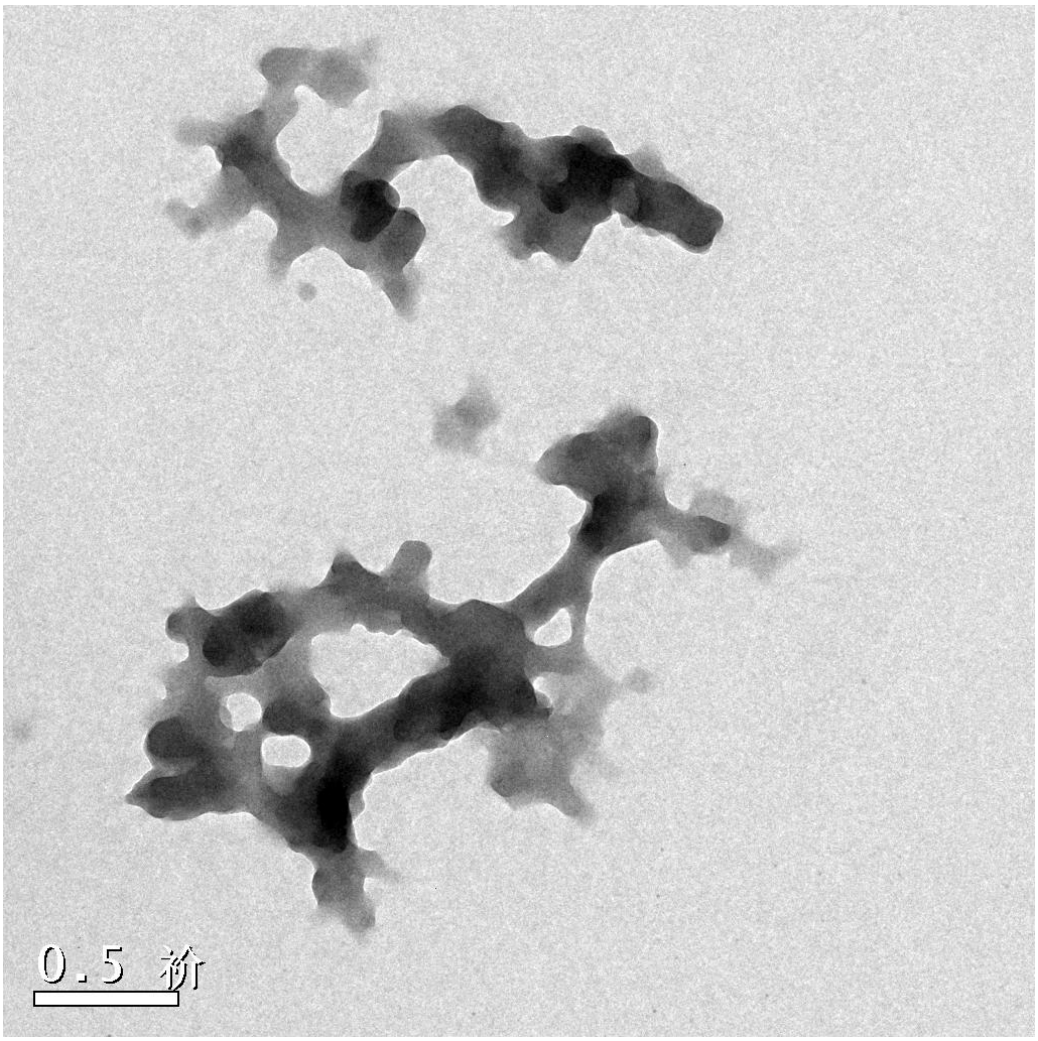

Figure S10. TEM images of suspension from interaction of **4** (10mM) with (*1R,2S*)-**7** (20mM) in cyclohexane and 1,2-dichloroethane of volume ratio 7:1.

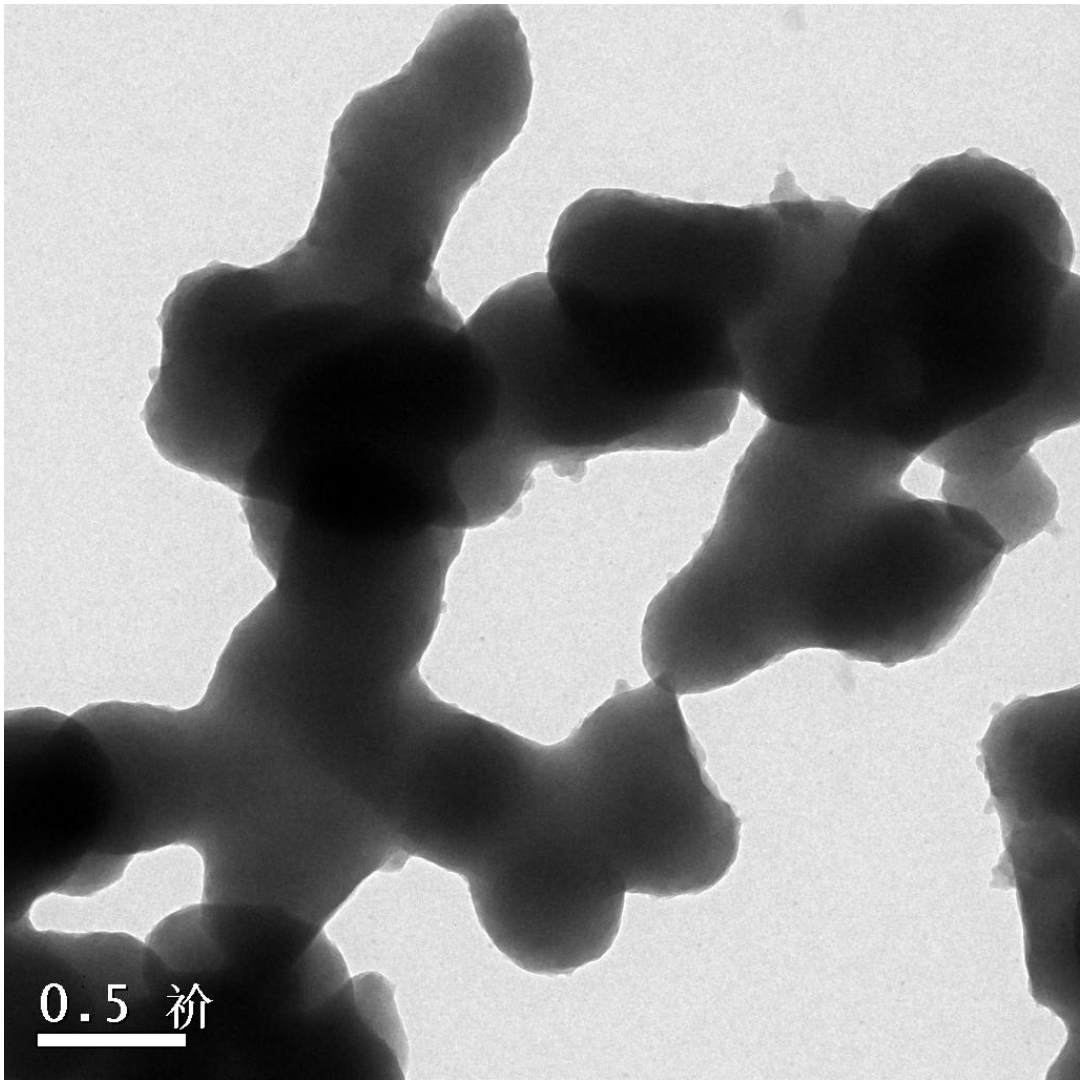

Figure S11. TEM images of suspension from interaction of **4** (10mM) with (*1S*,*2S*)-**8** (20mM) in cyclohexane and 1,2-dichloroethane of volume ratio 20:1.

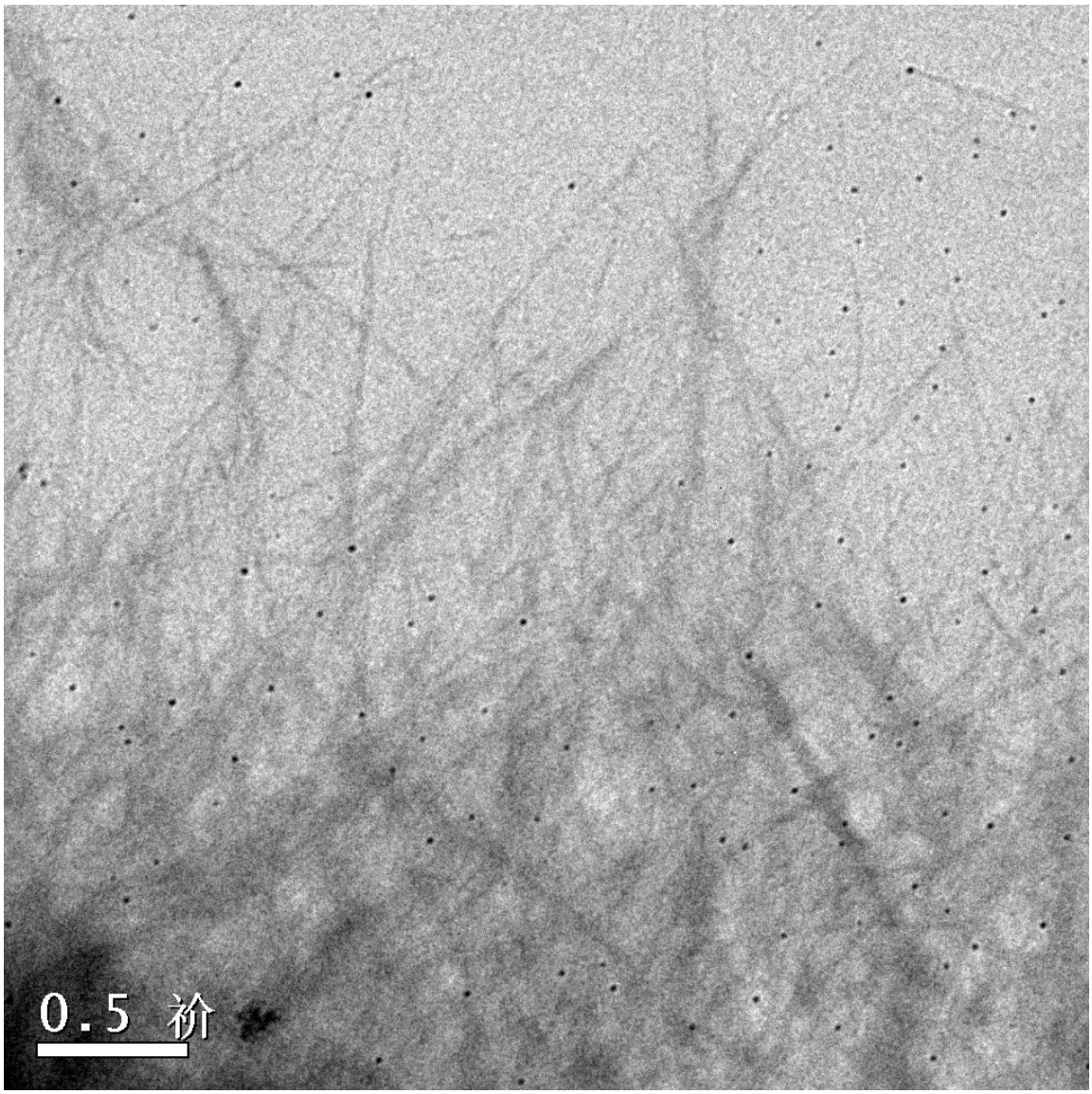

Figure S12. TEM images of gel from interaction of **4** (10mM) with (*1S,2S*)-**8** (20mM) in cyclohexane and 1,2-dichloroethane of volume ratio 20:1.

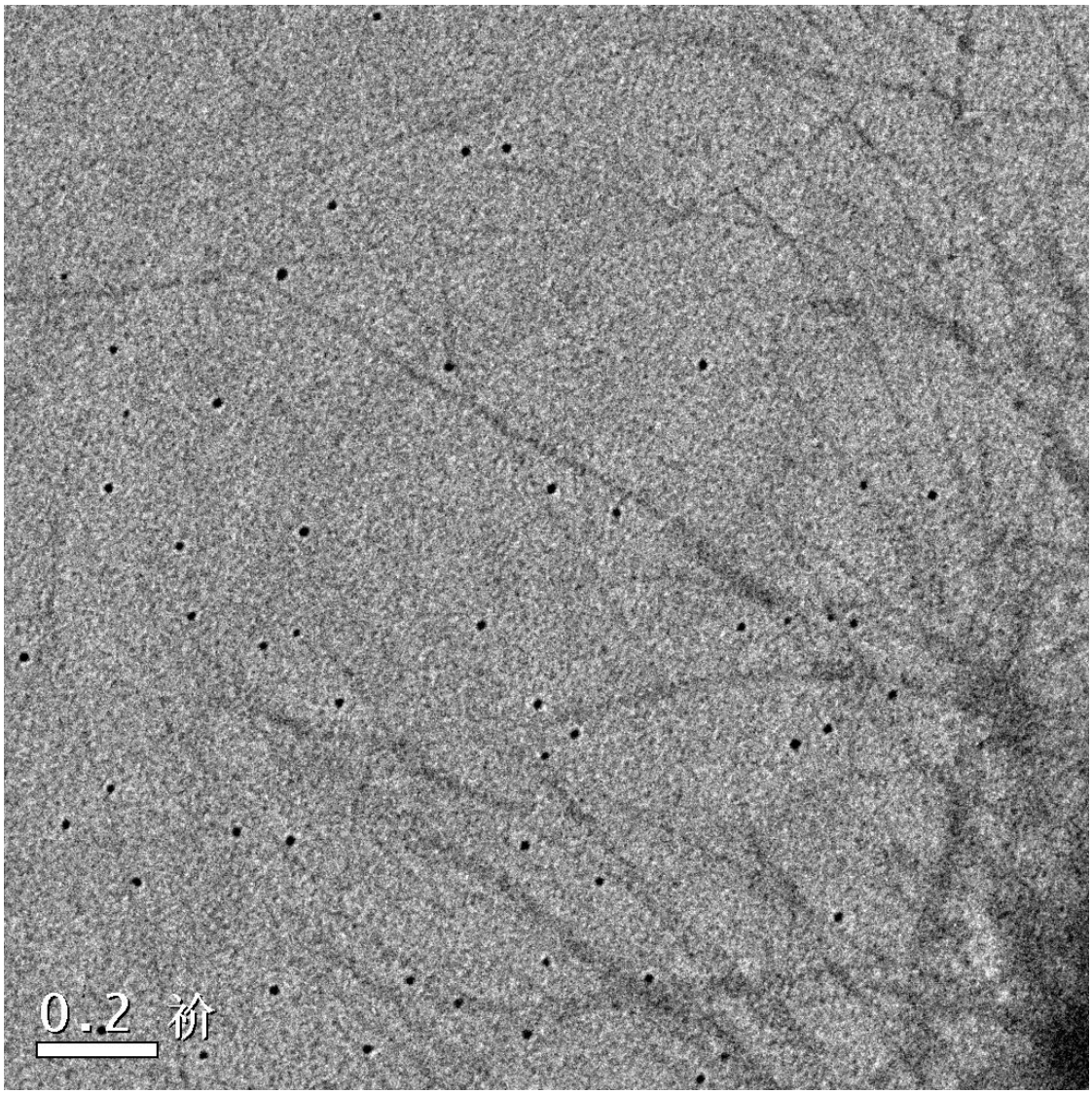

Figure S13. TEM images of gel from interaction of **4** (10mM) with (*1S*,*2S*)-**8** (20mM) in cyclohexane and 1,2-dichloroethane of volume ratio 20:1.

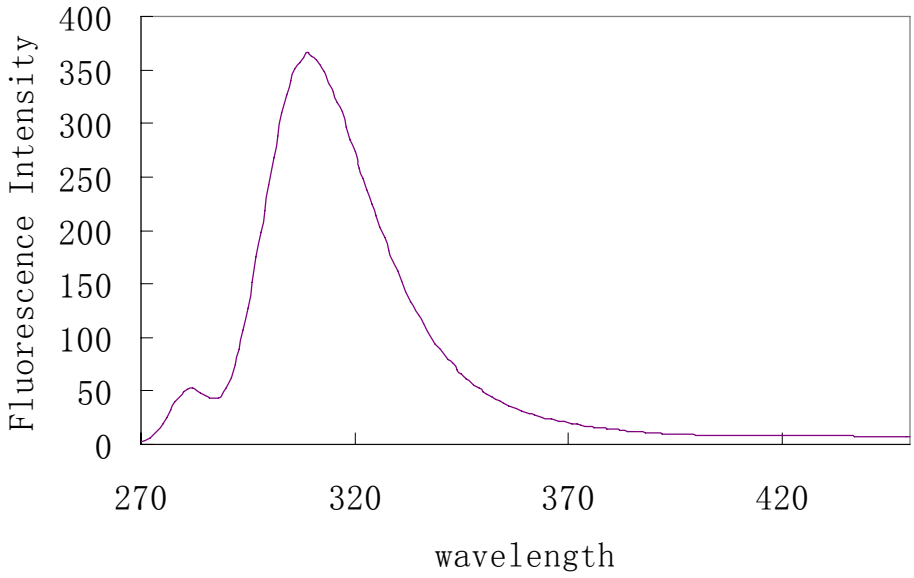

Figure S14. Emission spectra of **4** (1.0×10^{-4} M) in ethanol, λ_{em} = 280 nm, slit width: Ex 5 nm; Em 10 nm.

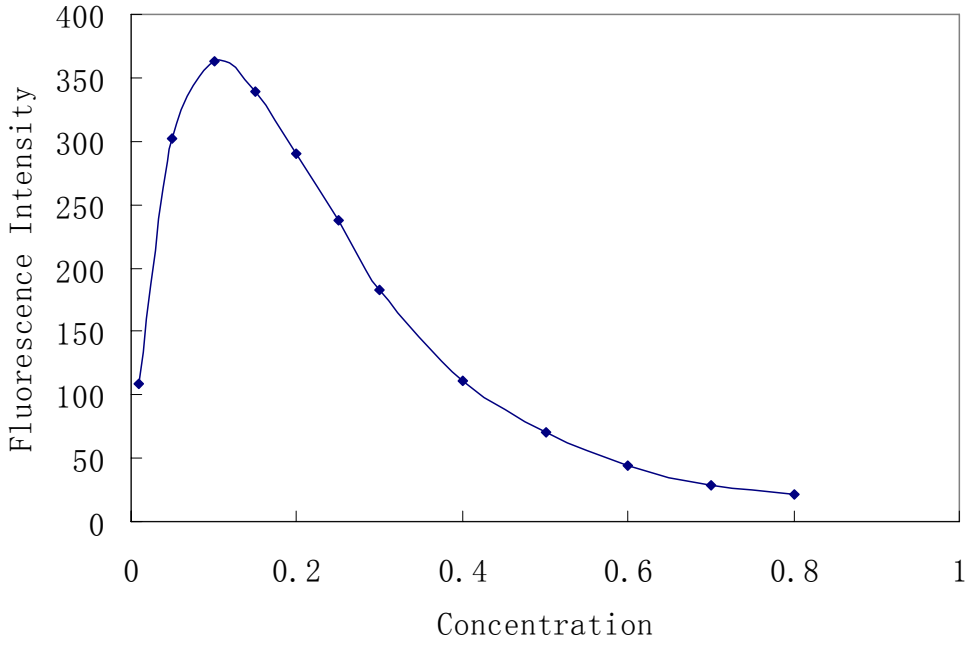

Figure S15. Changes of fluorescence intensity of **4** on its concentration ($c\times10^{3}$ Mol/L).

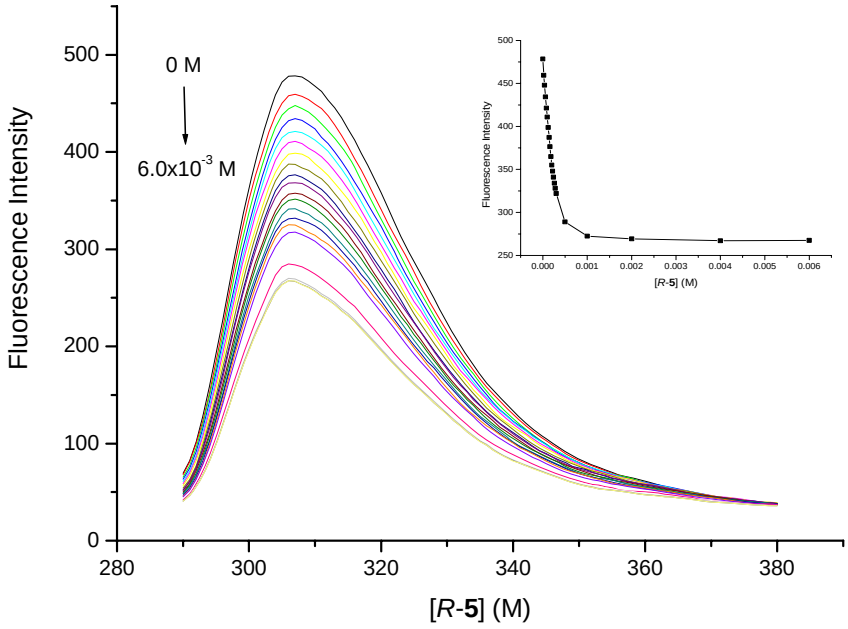

Figure S16. Emission spectra of **4** (1.0×10^{-4} M) on addition of (*R*)-**5** (0–6.0×10^{-3} M) in ethanol, λ_{ex} = 280 nm, slit width: Ex 5 nm; Em 5 nm. Inset: changes of fluorescence intensity at λ_{max} of **4** with molar concentration of (*R*)-**5**.

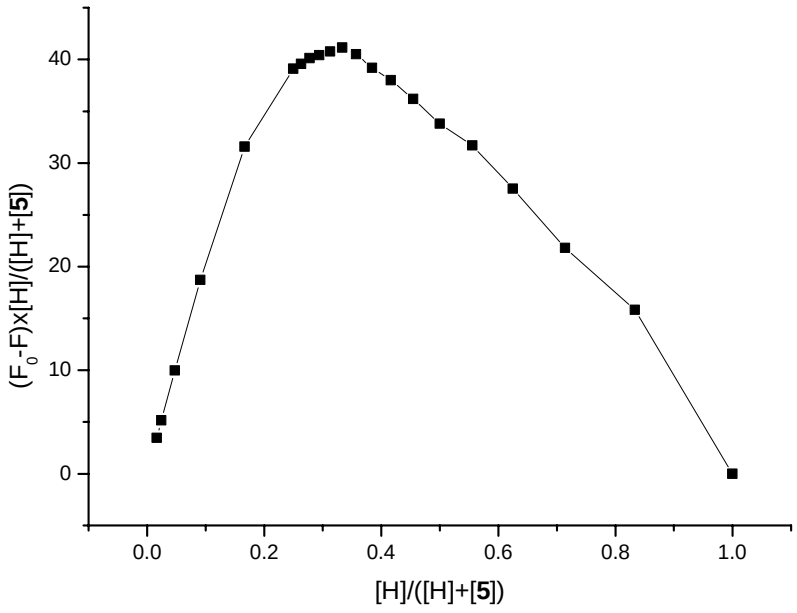

Figure S17. Job plot for fluorescence titration of **4** with *R*-**5**.

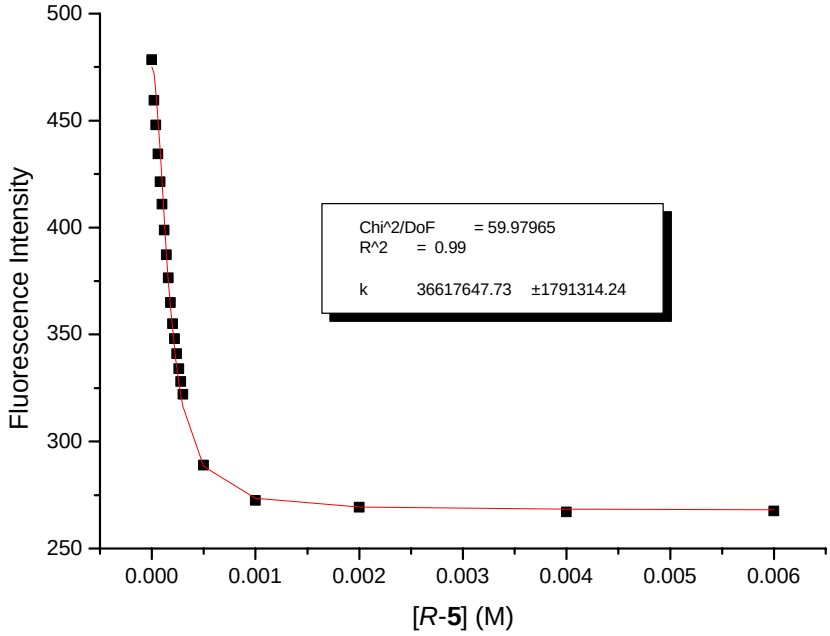

Figure S18. Determination of association constant by nonlinear fitting in Origin 6.1. The black squares are values by measurement and the red curve is one by fitting.

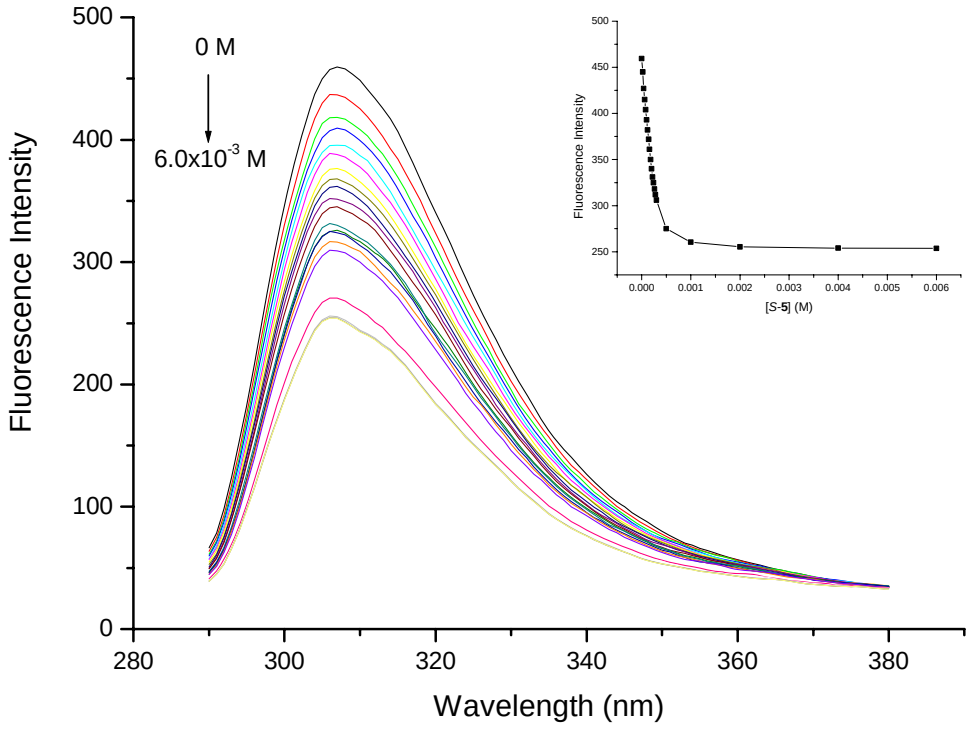

Figure S19. Emission spectra of **4** (1.0×10^{-4} M) on addition of (*S*)-**5** (0–6.0×10^{-3} M) in ethanol, λ_{ex} = 280 nm, slit width: Ex 5 nm; Em 5 nm. Inset: changes of fluorescence intensity at λ_{max} of **4** with molar concentration of (*S*)-**5**.

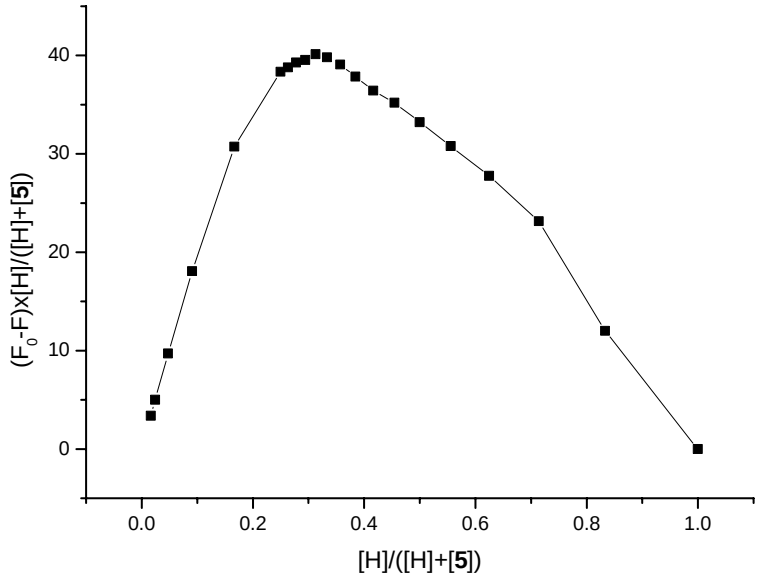

Figure S20. Job plot for fluorescence titration of **4** with *S*-**5**.

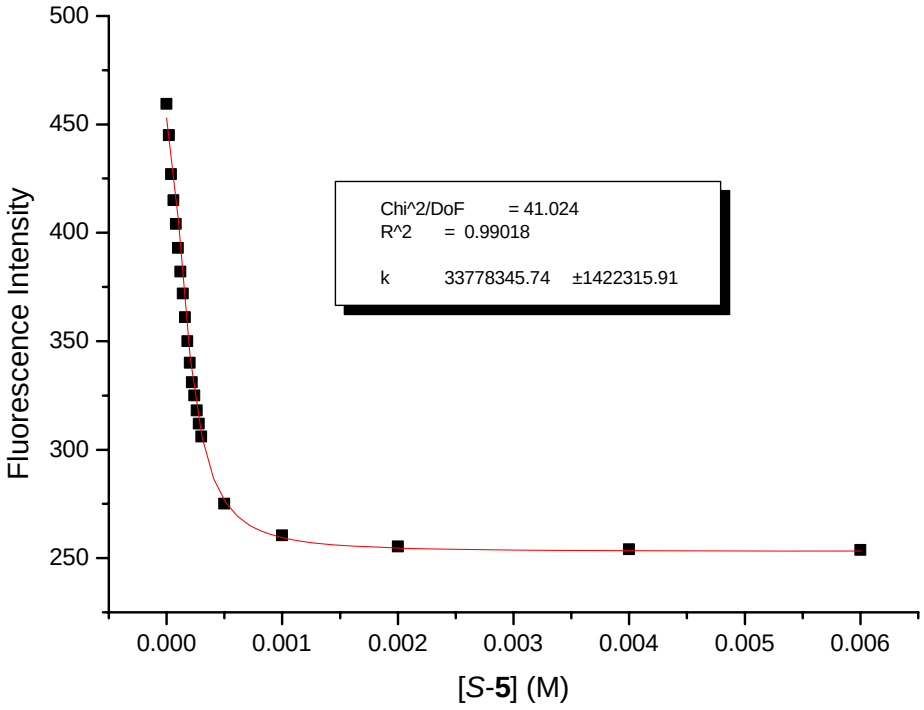

Figure S21. Determination of association constant by nonlinear fitting in Origin 6.1. The black squares are values by measurement and the red curve is one by fitting.

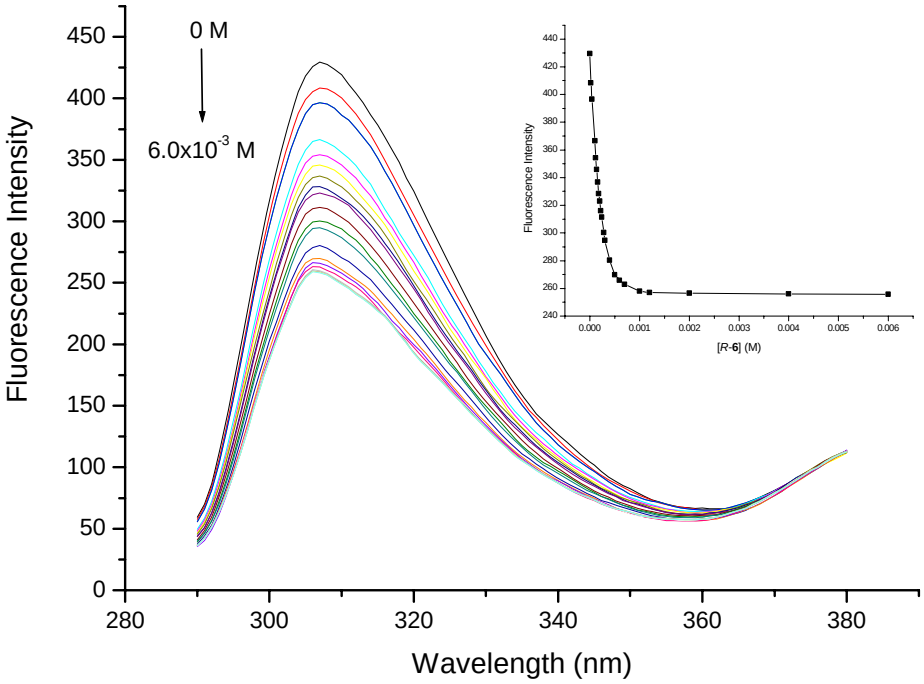

Figure S22. Emission spectra of **4** (1.0×10^{-4} M) on addition of (*R*)-**6** (0–6.0×10^{-3} M) in ethanol, λ_{ex} = 280 nm, slit width: Ex 5 nm; Em 5 nm. Inset: changes of fluorescence intensity at λ_{max} of **4** with molar concentration of (*R*)-**6**.

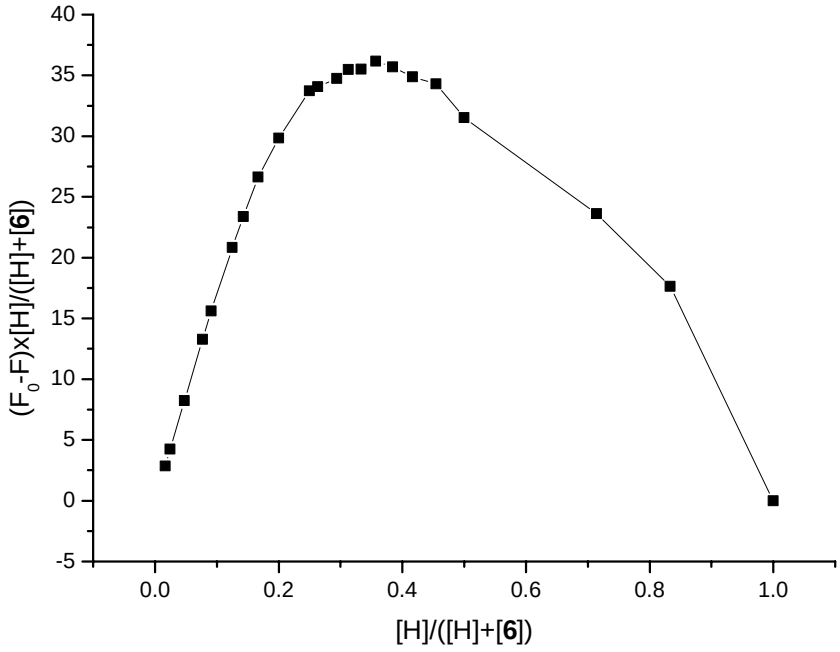

Figure S23. Job plot for fluorescence titration of **4** with *R*-**6**.

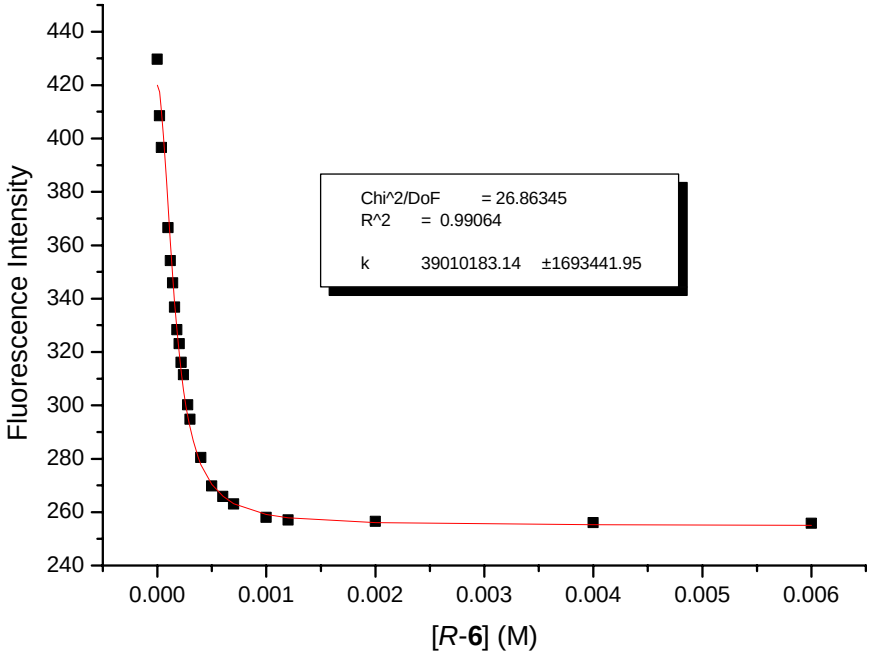

Figure S24. Determination of association constant by nonlinear fitting in Origin 6.1. The black squares are values by measurement and the red curve is one by fitting.

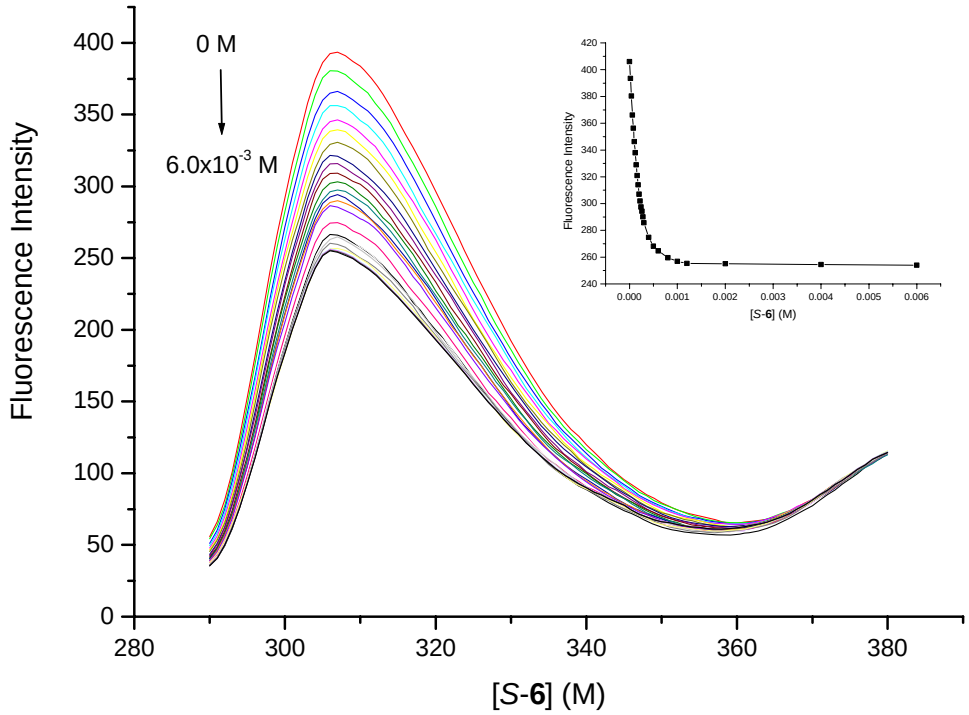

Figure S25. Emission spectra of **4** (1.0×10^{-4} M) on addition of (*S*)-**6** (0–6.0×10^{-3} M) in ethanol, λ_{ex} = 280 nm, slit width: Ex 5 nm; Em 5 nm. Inset: changes of fluorescence intensity at λ_{max} of **4** with molar concentration of (*S*)-**6**.

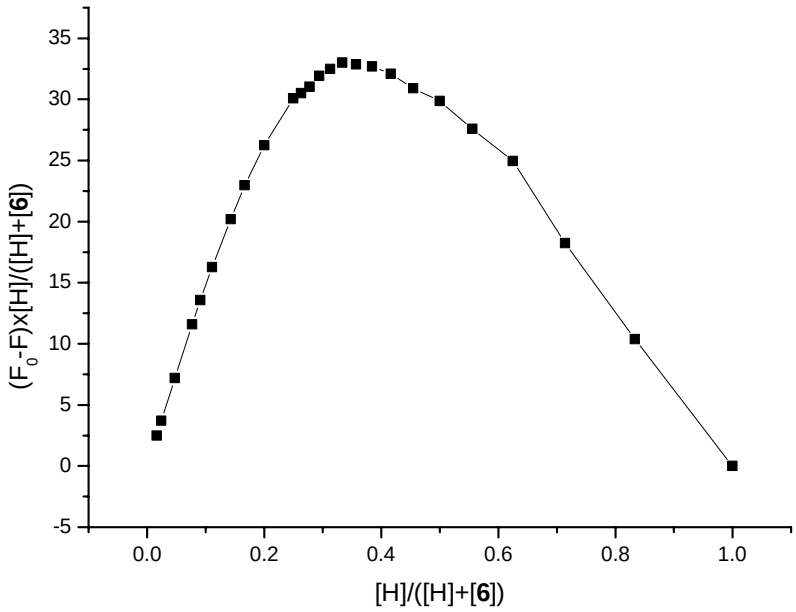

Figure S26. Job plot for fluorescence titration of **4** with *S*-**6**.

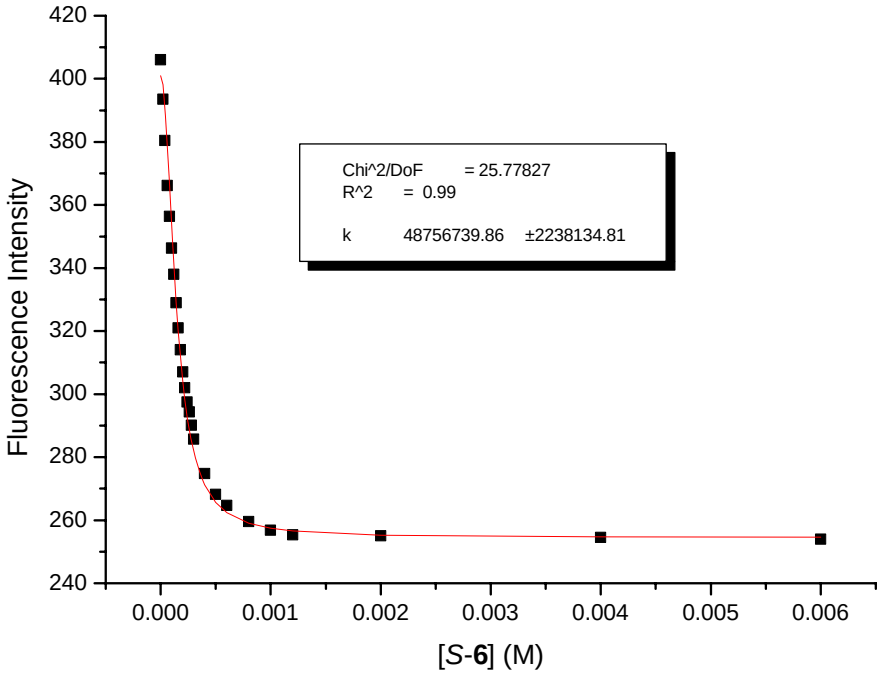

Figure S27. Determination of association constant by nonlinear fitting in Origin 6.1. The black squares are values by measurement and the red curve is one by fitting.

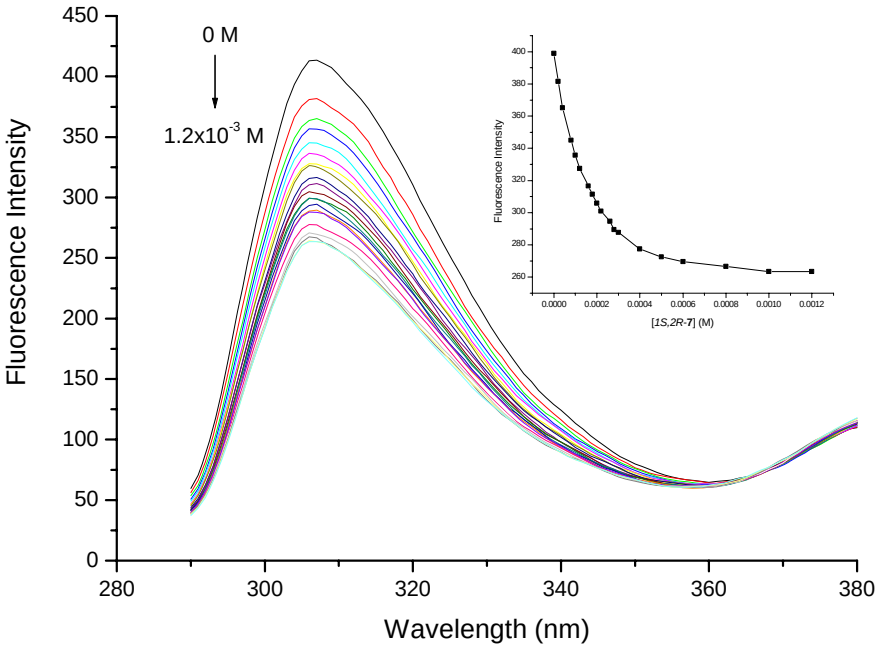

Figure S28. Emission spectra of **4** (1.0×10^{-4} M) on addition of (*1S,2R*)-**7** (0–1.2×10^{-3} M) in ethanol, λ_{ex} = 280 nm, slit width: Ex 5 nm; Em 5 nm. Inset: changes of fluorescence intensity at λ_{max} of **4** with molar concentration of (*1S,2R*)-**7**.

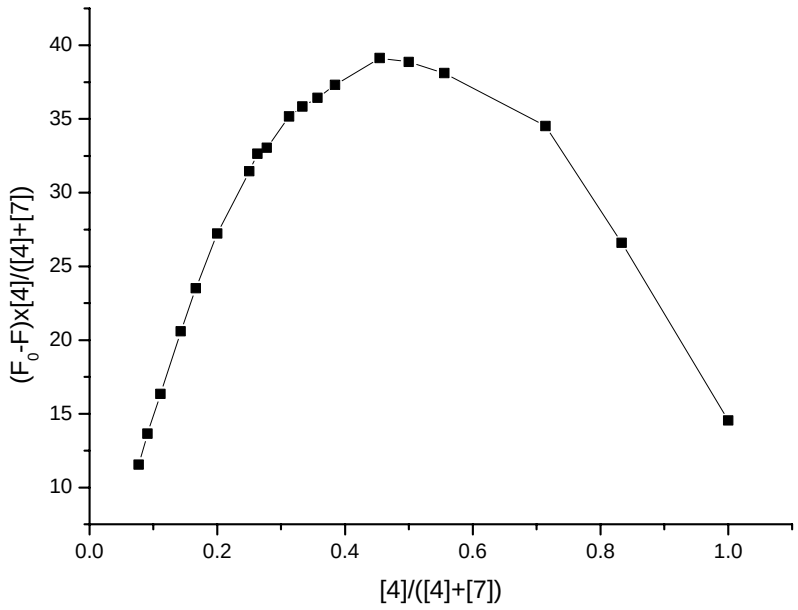

Figure S29. Job plot for fluorescence titration of **4** with (*1S,2R*)-**7**.

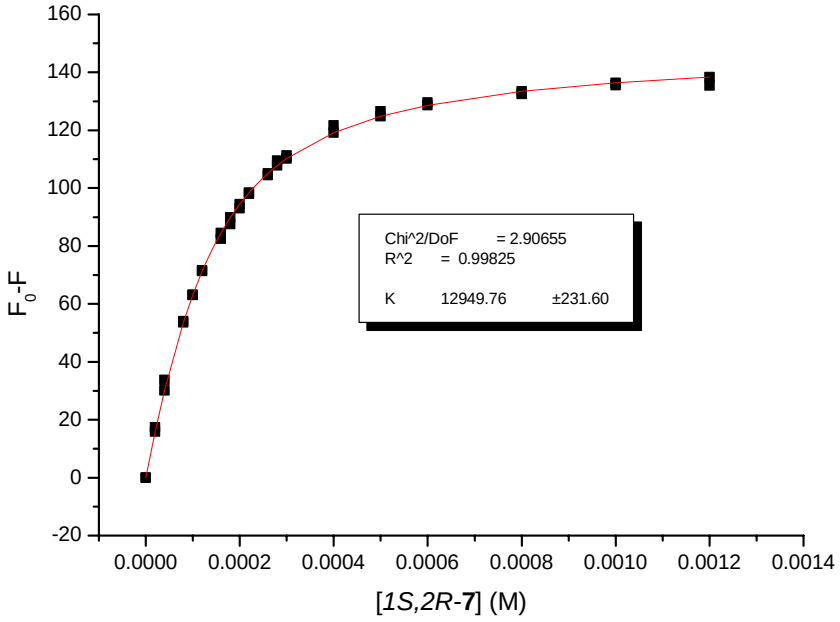

Figure S30. Determination of association constant by nonlinear fitting in Origin 6.1. The black squares are values by measurement and the red curve is one by fitting.

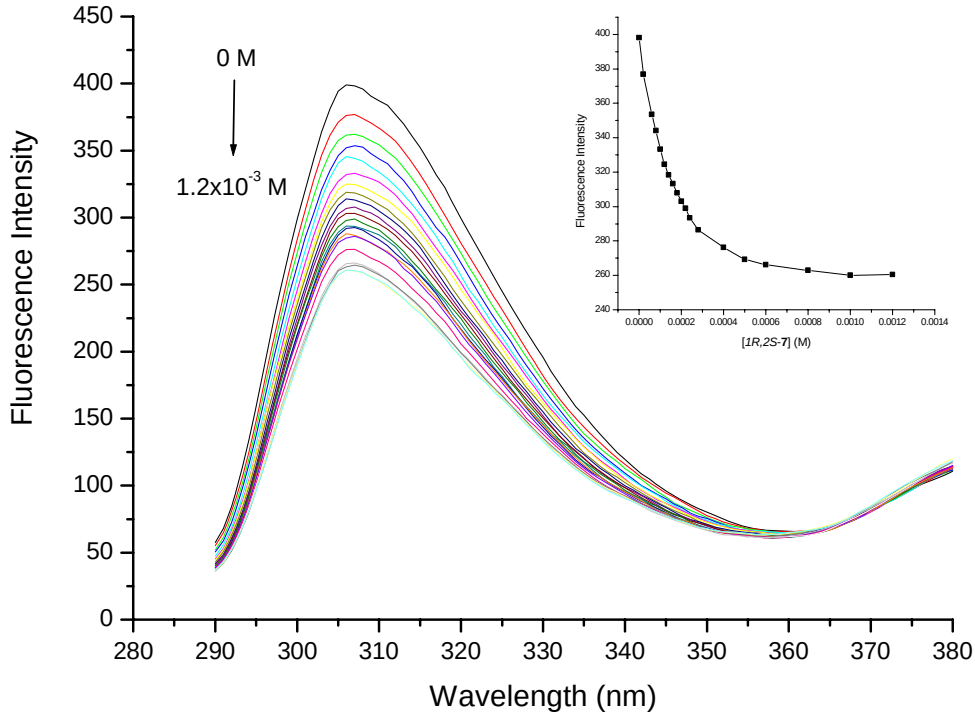

Figure S31. Emission spectra of **4** (1.0×10^{-4} M) on addition of (*1R,2S*)-**7** (0–1.2×10^{-3} M) in ethanol, λ_{ex} = 280 nm, slit width: Ex 5 nm; Em 5 nm. Inset: changes of fluorescence intensity at λ_{max} of **4** with molar concentration of (*1R,2S*)-**7**.

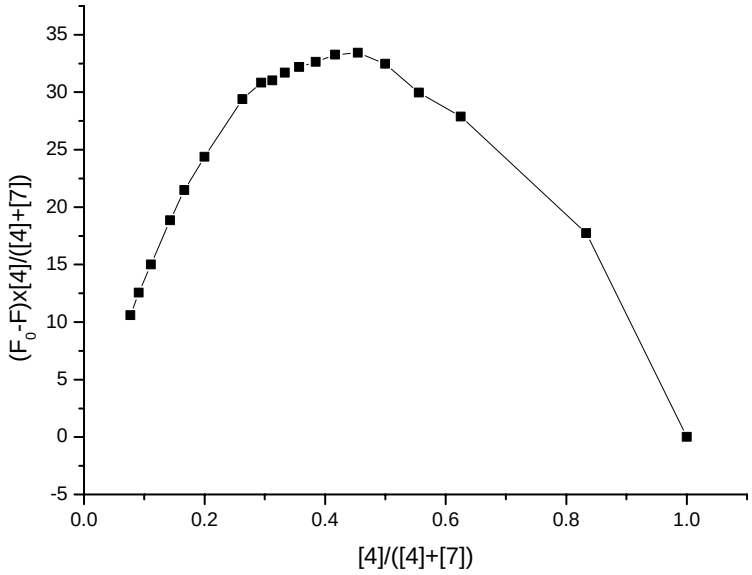

Figure S32. Job plot for fluorescence titration of **4** with (*1R,2S*)-**7**.

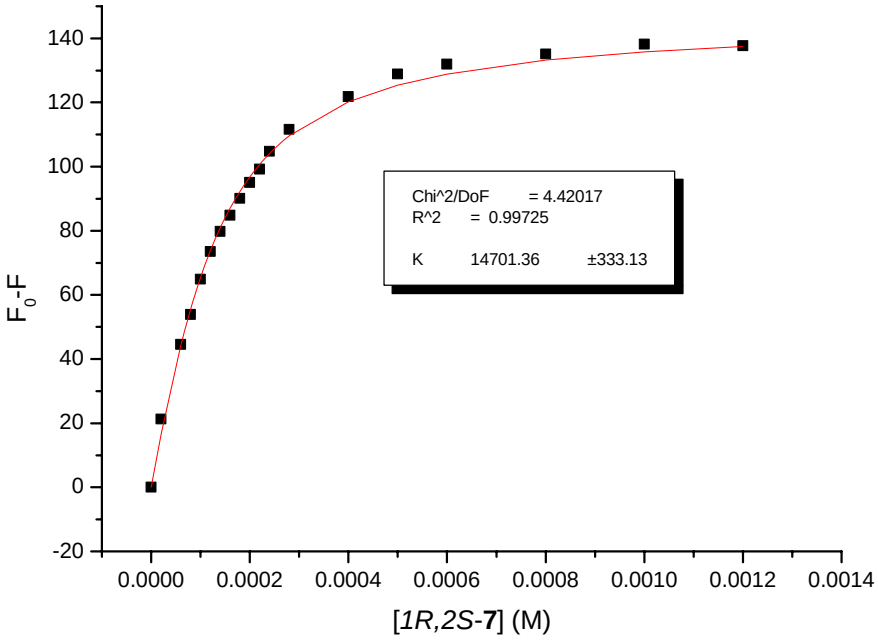

Figure S33. Determination of association constant by nonlinear fitting in Origin 6.1. The black squares are values by measurement and the red curve is one by fitting.

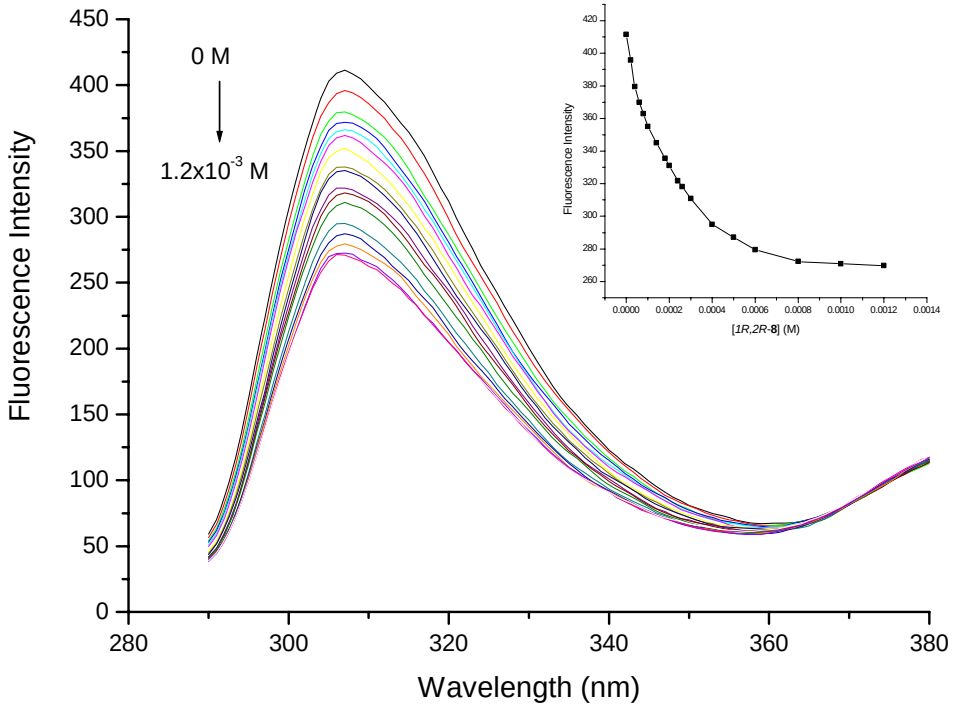

Figure S34. Emission spectra of **4** (1.0×10^{-4} M) on addition of (*1R,2R*)-**8** (0–1.2×10^{-3} M) in ethanol, λ_{ex} = 280 nm, slit width: Ex 5 nm; Em 5 nm. Inset: changes of fluorescence intensity at λ_{max} of **4** with molar concentration of (*1R,2R*)-**8**.

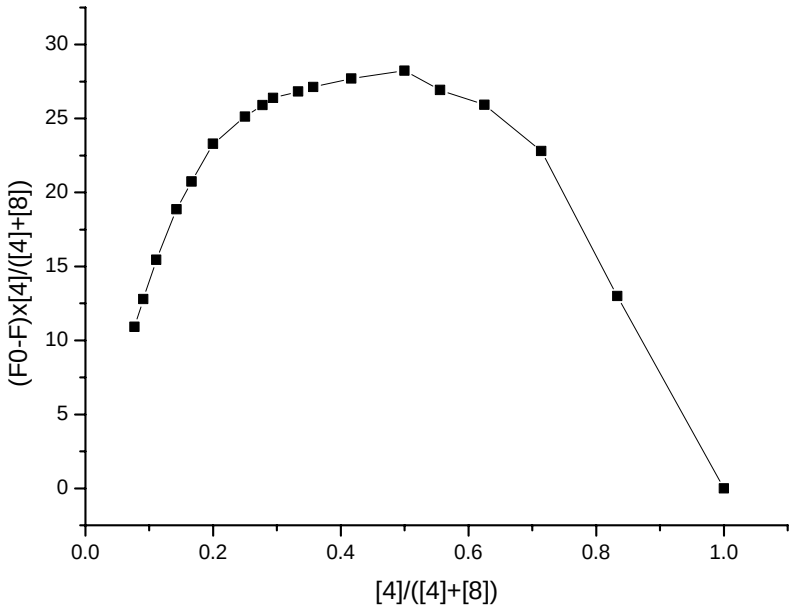

Figure S35. Job plot for fluorescence titration of **4** with (*1R,2R*)-**8**.

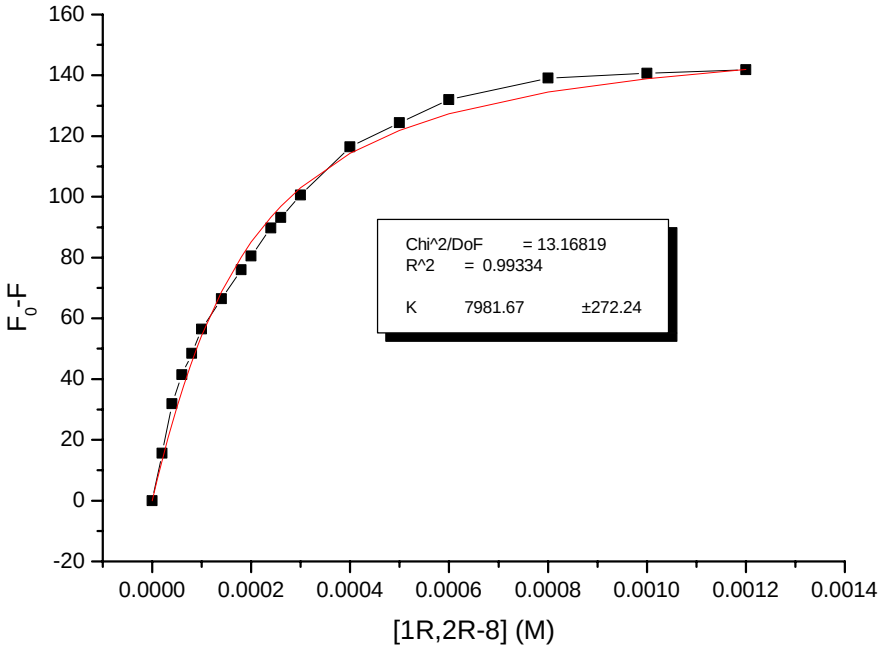

Figure S36. Determination of association constant by nonlinear fitting in Origin 6.1. The black squares are values by measurement and the red curve is one by fitting.

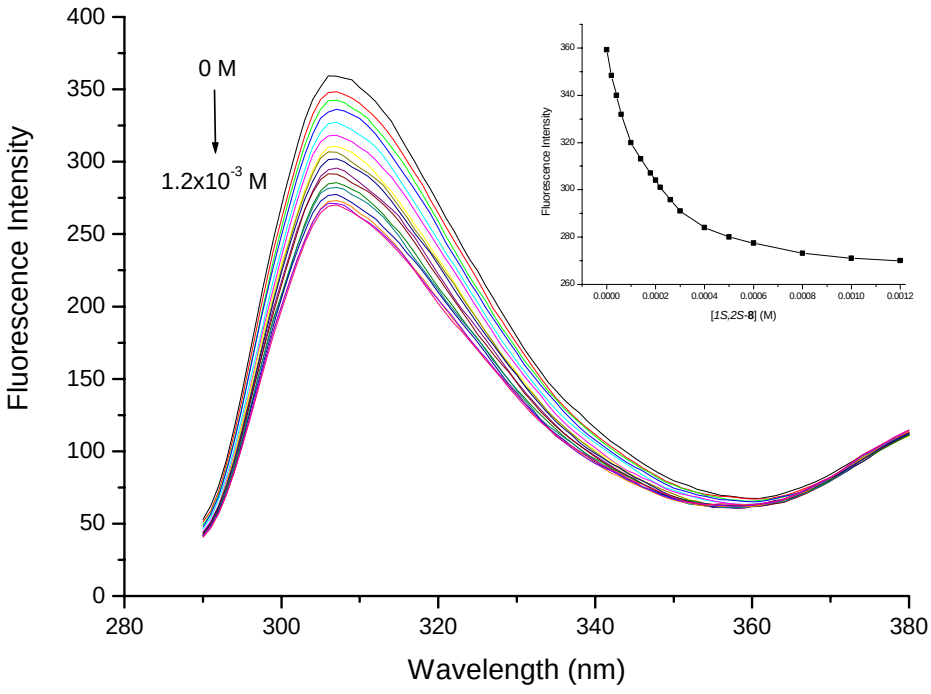

Figure S37. Emission spectra of **4** (1.0×10^{-4} M) on addition of (*1S,2S*)-**8** (0–1.2×10^{-3} M) in ethanol, λ_{ex} = 280 nm, slit width: Ex 5 nm; Em 5 nm. Inset: changes of fluorescence intensity at λ_{max} of **4** with molar concentration of (*1S,2S*)-**8**.

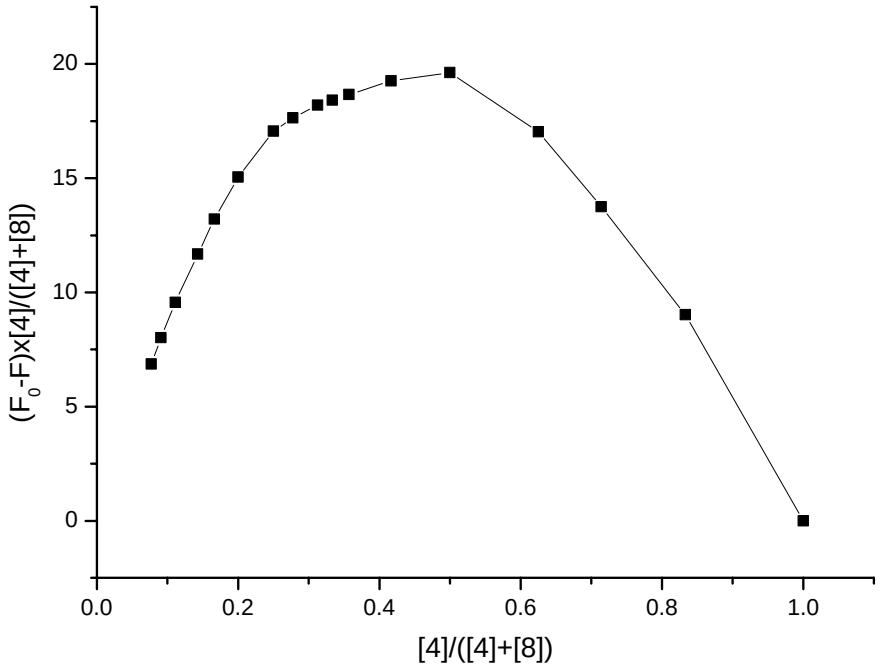

Figure S38. Job plot for fluorescence titration of **4** with (*1S,2S*)-**8**.

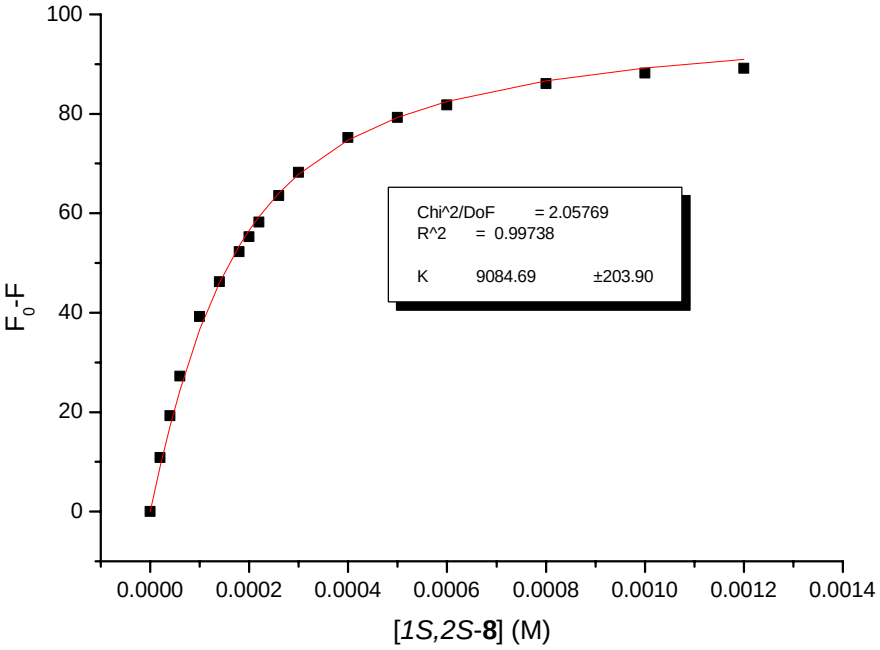

Figure S39. Determination of association constant by nonlinear fitting in Origin 6.1. The black squares are values by measurement and the red curve is one by fitting.